Geophys. J. Int. (2006) **164,** 99–108 doi: 10.1111/j.1365-246X.2005.02807.x

Correcting for bias due to noise in coda wave interferometry

Huub Douma and Roel Snieder

Center for Wave Phenomena, Colorado School of Mines, Golden, CO 80401-1887, *USA. E-mail: huub@dix.mines.edu*

Accepted 2005 September 13. Received 2005 September 11; in original form 2004 November 17

SUMMARY

Coda wave interferometry (CWI) utilizes multiply scattered waves to diagnose small changes in a medium by using the scattering medium as an interferometer. Since the medium is usually stationary over the duration of a seismic experiment, different (non-overlapping) time windows in the coda allow for independent estimates of the medium perturbation. If the seismograms are contaminated with noise, only those time windows can be used for which the amplitude of the coda is significantly above the ambient noise level. This limits the usable number of independent time windows. Here, we show how bias due to noise in CWI can be accounted for, by deriving a correction factor for the cross-correlation coefficient, under the assumptions that the stochastic processes underlying the noise realizations in both signals are mutually uncorrelated and stationary with zero mean. This correction factor allows more time windows further into the decaying coda to be used, and hence allows for a reduction of the error bars on the medium perturbation estimates. We demonstrate the validity of this correction factor by using data from a numerical experiment and field measurements. These experiments involve the displacement of point scatterers and a change in the source location, respectively. The application of our correction factor is not limited to CWI, but can be used to correct for bias induced by noise in any application that uses cross-correlation between different signals that are contaminated with noise.

Key words: cross-correlation, earthquake location, monitoring, noise, scattering, seismic coda.

1 INTRODUCTION

Multiply scattered wavefields have been experimentally shown to be remarkably stable with respect to perturbations of the boundary conditions of experiments with multiply scattered waves (Derode *et al.* 1995, 1999). Due to this stability, the information carried by multiply scattered waves has been successfully used in an industrial context (e.g. Fink 1997). Coda wave interferometry (Roberts *et al.* 1992; Snieder *et al.* 2002; Snieder 2002; Grêt *et al.* 2005b; Snieder 2004) uses multiply scattered waves to detect small changes by using the scattering medium as an interferometer. Since multiply scattered waves dominate the final portions of a seismogram, they are usually referred to as coda waves just as, in musical notation, the coda denotes the closing part of a musical piece. Hence the name *coda wave interferometry* (CWI). Since CWI uses multiply scattered waves, it is inherently more sensitive to changes in the medium than are techniques based on single scattering, as multiply scattered waves sense changes in the medium multiple times.

In parallel, but independently, diffusing acoustic wave spectroscopy (DAWS) (Page *et al.* 2000; Cowan *et al.* 2002) was developed as the classical equivalent of diffusing wave spectroscopy (DWS) (Maret & Wolf 1987; Pine *et al.* 1988; Yodh *et al.* 1990; Weitz & Pine 1993). In DWS light is used to study different aspects of strongly scattering media, whereas in DAWS classical waves are used to probe such media. DWS has been used in many applications such as, for example, determining the aging of foams, particle sizing, and determining the motion of particles in fluidized suspensions on ångström length scales (Weitz & Pine 1993). So far, DAWS has mainly been used to determine the relative mean square displacement of fluidized suspensions of particles (Page *et al.* 1999; Cowan *et al.* 2000; Page *et al.* 2000; Cowan *et al.* 2002). CWI has been succesfully used to measure the non-linear dependence of seismic velocity in rocks on temperature (Snieder *et al.* 2002), to monitor volcanoes (Grêt *et al.* 2005a), and to estimate source displacement (Snieder & Vrijlandt 2005). The ability to use CWI to determine the relative mean square displacement of point scatterers from noise-free waveforms was established using a numerical experiment by Snieder *et al.* (2002). Both CWI and DAWS use the amplitude information as well as the phase information of the multiply scattered wavefields, and are both based on a path summation approach to model the multiply scattered wavefields. Hence, both methods are in principle the same, but have been used for different applications.

CWI is based on a measure of cross-correlation between multiply scattered wavefields recorded before and after a medium has changed. The cross-correlation coefficients calculated for different (non-overlapping) time windows provide independent estimates of the medium perturbations. These independent estimates in turn allow for the calculation of error estimates of the perturbation; the larger the number of independent (unbiased) measurements, the smaller the error estimates.

When the coda is contaminated with noise, the number of independent time windows that can be used is limited to traveltimes where the ambient noise level is small compared to the amplitudes of the multiply scattered waves. To be able to use as many independent time windows as possible, and hence reduce the error bars on the inferred perturbation, it is important to correct the cross-correlation function for the bias caused by noise. In this paper, we show how this bias in CWI can be corrected for, by deriving a correction factor for the cross-correlation coefficient based on the assumptions that the stochastic processes underlying the noise realizations in both signals, are mutually uncorrelated and stationary with zero mean. We demonstrate its validity by using data from a numerical experiment involving the displacement of point scatterers, and field data involving the displacement of the source location.

The organization of this paper is as follows. We briefly state the essence of CWI and derive the noise-correction factor. Subsequently we show the validity of the correction factor using the numerical and field experiments mentioned above. We conclude with a short discussion of the results. In Appendix A we derive a condition for the reliability of the correction factor for the zero-lag cross-correlation coefficient. This condition can be used to determine the time windows in the coda where the correction factor is reliable.

2 CODA WAVE INTERFEROMETRY

Here, we summarize the essence of CWI, but refer to Snieder (2006) and references therein, for a treatment of the theory leading to the expressions presented here.

In CWI, we measure the normalized cross-correlation between seismograms $u_u(t)$ and $u_p(t)$, where $u_u(t)$ and $u_p(t)$ are the wavefields recorded at the same location from an unperturbed and perturbed medium, respectively. We aim to infer the level of the perturbation in the medium from this correlation. The normalized time-shifted cross-correlation is calculated as the time-windowed correlation coefficient $r(t_s; t, t_w)$, given by

$$r(t_s; t, t_w) := \frac{(u_u, u_p)_{(t_s; t, t_w)}}{\sqrt{(u_u, u_u)_{(t_s=0; t, t_w)}(u_p, u_p)_{(t_s=0; t, t_w)}}}, \tag{1}$$

with

$$(u_u, u_p)_{(t_s; t, t_w)} := \frac{1}{2t_w}\int_{t-t_w}^{t+t_w} u_u(t')u_p(t'+t_s)\,dt',$$

where t_s is the time-shift in the cross-correlation, t is the central window time, and t_w is half the duration of the time window. Assuming the perturbation in the medium mainly influences the traveltimes of the waves with a resulting time-shift τ_T for the wave that travels along trajectory T (Snieder 2006), the maximum value of the correlation coefficient, max $[r(t_s; t, t_w)]$, is related to the variance of the traveltime perturbations σ_τ^2 by

$$\max[r(t_s; t, t_w)] = 1 - \frac{1}{2}\overline{\omega^2}\sigma_\tau^2, \tag{2}$$

where the frequency $\overline{\omega^2}$ is given by

$$\overline{\omega^2} := \frac{\int_{t-t_w}^{t+t_w} \dot{u}_u^2(t')\,dt'}{\int_{t-t_w}^{t+t_w} u_u^2(t')\,dt'}, \tag{3}$$

and σ_τ^2 is defined as

$$\sigma_\tau^2 := \frac{\sum_T A_T^2(\tau_T - \langle\tau\rangle)^2}{\sum_T A_T^2}. \tag{4}$$

In eq. (4), $\dot{u}$ denotes the time derivative of $u(t)$, A_T^2 is the intensity of the wave that has travelled along trajectory T, and $\langle\tau\rangle$ denotes the intensity-weighted traveltime perturbation averaged over all scattering paths. It turns out that for the perturbations studied in this paper, that is, small displacement of the scatterers and a change in the source location, the assumption that the perturbation mainly influences the traveltimes, is appropriate. Note that in eq. (2), as well as throughout the remainder of this paper, the maximum is calculated with respect to t_s for given values of t and t_w.

3 CORRECTING FOR THE BIAS DUE TO NOISE

In eq. (2), the waveforms $u_u(t)$ and $u_p(t)$ used to calculate max $[r(t_s; t, t_w)]$ are assumed to be free of noise. To study the influence of noise on CWI, we derive a correction factor for the correlation coefficient when the waveforms $u_u(t)$ and $u_p(t)$ are contaminated with noise. We define

$$u'_u(t) := u_u(t) + n_u(t)\,, \quad u'_p(t) := u_p(t) + n_p(t), \tag{5}$$

where $u'_u(t)$ and $u'_p(t)$ are the noise-contaminated signals, $u_u(t)$ and $u_p(t)$ the noise-free waveforms, and $n_u(t)$ and $n_p(t)$ the noise signals for the unperturbed and perturbed wavefields, respectively. Using the noise-contaminated signals, we define the noise-contaminated cross-correlation

coefficient as

$$r'(t_s; t, t_w) = \frac{(u'_u, u'_p)_{(t_s;t,t_w)}}{\sqrt{(u'_u, u'_u)_{(t_s=0;t,t_w)}(u'_p, u'_p)_{(t_s=0;t,t_w)}}}. \tag{6}$$

Our aim is to derive a correction factor $c(t_s; t, t_w)$ such that

$$r(t_s; t, t_w) \approx c(t_s; t, t_w) r'(t_s; t, t_w). \tag{7}$$

Throughout the remaining derivation, we assume that the noise signals $n_u(t)$ and $n_p(t)$ are realizations of mutually uncorrelated stationary stochastic processes with zero mean. Stationarity is here meant in the wide sense, that is, the mean is the same (zero) for all times, and the autocorrelation depends only on the time-shift t_s (Papoulis 1991, p. 298).

Using eq. (5), we find

$$(u'_u, u'_p)_{(t_s;t,t_w)} = (u_u, u_p)_{(t_s;t,t_w)} + (u_u, n_p)_{(t_s;t,t_w)} + (u_p, n_u)_{(t_s;t,t_w)} + (n_u, n_p)_{(t_s;t,t_w)}, \tag{8}$$

$$(u'_u, u'_u)_{(t_s=0;t,t_w)} = (u_u, u_u)_{(t_s=0;t,t_w)} + 2(u_u, n_u)_{(t_s=0;t,t_w)} + (n_u, n_u)_{(t_s=0;t,t_w)}, \tag{9}$$

$$(u'_p, u'_p)_{(t_s=0;t,t_w)} = (u_p, u_p)_{(t_s=0;t,t_w)} + 2(u_p, n_p)_{(t_s=0;t,t_w)} + (n_p, n_p)_{(t_s=0;t,t_w)}. \tag{10}$$

In eqs (8)–(10), terms of the form $(u, n)_{(t_s;t,t_w)}$ appear, where $u = u(t)$ is a deterministic signal and $n = n(t)$ a realization of a stochastic process $\boldsymbol{n}(t)$.[1] These terms are time-windowed averages of the product $x(t) := u(t)n(t + t_s)$, where $u(t)$ is deterministic. Hence, $x(t)$ is a single realization of a stochastic process $\boldsymbol{x}(t)$ with the same statistical properties as $\boldsymbol{n}(t)$. Since we are dealing with windowed time averages of single realizations of stochastic processes, we want to evaluate the time averages using the underlying ensemble averages. This leads us to the ergodicity of the stochastic signals treated here.

It is known (Papoulis 1991, chapter 13-1) that a (stationary) stochastic process $\boldsymbol{x}(t)$ is mean-ergodic if and only if $A(T) := (\int_0^T C_{\boldsymbol{xx}}(\tau)\,\mathrm{d}\tau)/T \to 0$ as $T \to \infty$, where $C_{\boldsymbol{xx}}(\tau)$ is the autocovariance of $\boldsymbol{x}(t)$ at time-shift τ; this is Slutsky's theorem. For $A(T) \to 0$ as $T \to \infty$, it is sufficient for $C_{\boldsymbol{xx}}(\tau) \to 0$ as $\tau \to \infty$. This means that $\boldsymbol{x}(t)$ and $\boldsymbol{x}(t + \tau)$, and thus $\boldsymbol{n}(t)$ and $\boldsymbol{n}(t + \tau)$, must be uncorrelated for large time-shifts τ, a requirement that is a reasonable assumption in most practical applications. Hence, with this assumption, we can conclude that $\boldsymbol{x}(t)$ is mean-ergodic, meaning that the time average $(\int_{-T}^{T} x(t)\,dt)/(2T)$, that is, the time average of a single realization $x(t)$, is close to $E(\boldsymbol{x}(t)) = 0$ with probability close to 1. Here, $E(\boldsymbol{x}(t))$ denotes the expected value of $\boldsymbol{x}(t)$. We have $E(\boldsymbol{x}(t)) = 0$ since $\boldsymbol{x}(t)$ has the same statistical properties as $\boldsymbol{n}(t)$, that is, zero mean. In turn, this means that

$$(u, n)_{(t_s;t,t_w)} = \frac{1}{2t_w}\int_{t-t_w}^{t+t_w} u(t')n(t' + t_s)\,dt' \approx 0, \tag{11}$$

provided the window length t_w is at least several dominant periods of the noise-contaminated signal. Note that the only real restrictive requirement used to show eq. (11), is that $\boldsymbol{n}(t)$ is stationary with zero mean.

For the term $(n_u, n_p)_{(t_s;t,t_w)}$ in eqs (8)–(10), we follow a similar argument, except that now the stochastic process to be considered is $\boldsymbol{z}(t) := \boldsymbol{n}_u(t)\boldsymbol{n}_p(t + t_s)$, where $\boldsymbol{n}_u(t)$ and $\boldsymbol{n}_p(t)$ are the underlying stochastic processes of which $n_u(t)$ and $n_p(t)$, respectively, are single realizations. As in the previous paragraph, for $\boldsymbol{z}(t)$ to be mean ergodic, it is sufficient if $C_{\boldsymbol{zz}}(\tau) \to 0$ as $\tau \to \infty$. Since $\boldsymbol{n}_u(t)$ and $\boldsymbol{n}_p(t)$ are assumed to be mutually uncorrelated with both zero mean, it follows that $C_{\boldsymbol{zz}}(\tau) = C_{\boldsymbol{n_u n_u}}(\tau)C_{\boldsymbol{n_p n_p}}(\tau)$. Again, under the often practical assumption that $\boldsymbol{n}_u(t)$ and $\boldsymbol{n}_p(t + \tau)$, as well as $\boldsymbol{n}_p(t)$ and $\boldsymbol{n}_p(t + \tau)$, are uncorrelated for large τ, we have that $C_{\boldsymbol{n_u n_p}}(\tau) \to 0$ and $C_{\boldsymbol{n_p n_p}}(\tau) \to 0$ as $\tau \to \infty$, and hence $C_{\boldsymbol{zz}}(\tau) \to 0$ as $\tau \to \infty$. This means that $\boldsymbol{z}(t)$ is mean ergodic, which is equivalent to $\boldsymbol{n}_u(t)$ and $\boldsymbol{n}_p(t)$ being cross-covariance ergodic. Therefore, we have that $(\int_{-T}^{T} z(t)\,dt)/(2T)$ is close to $E(\boldsymbol{z}(t)) = E(\boldsymbol{n}_u(t)\,\boldsymbol{n}_p(t + t_s)) = E(\boldsymbol{n}_u(t))E(\boldsymbol{n}_p(t + t_s)) = 0$ with probability close to 1. This implies that we have

$$(n_u, n_p)_{(t_s;t,t_w)} = \frac{1}{2t_w}\int_{t-t_w}^{t+t_w} n_u(t')n_p(t' + t_s)\,dt' \approx 0, \tag{12}$$

with the same assumption for the window length t_w as used in eq. (11). Note that both approximations (11) and (12) become more accurate with increasing window lengths.

Using eqs (11) and (12) in eqs (8)–(10), it follows that

$$(u'_u, u'_p)_{(t_s;t,t_w)} \approx (u_u, u_p)_{(t_s;t,t_w)}, \tag{13}$$

$$(u'_u, u'_u)_{(t_s=0;t,t_w)} \approx (u_u, u_u)_{(t_s=0;t,t_w)} + (n_u, n_u)_{(t_s=0;t,t_w)}, \tag{14}$$

$$(u'_p, u'_p)_{(t_s=0;t,t_w)} \approx (u_p, u_p)_{(t_s=0;t,t_w)} + (n_p, n_p)_{(t_s=0;t,t_w)}. \tag{15}$$

[1] Throughout this paper we adopt the notation that $n(t)$ denotes a realization of an underlying stochastic process $\boldsymbol{n}(t)$.

Using these approximations in eq. (6), and substituting the resulting expression in eq. (7), it follows that the correction factor $c(t_s; t, t_w)$ is given by

$$c(t_s; t, t_w) \approx \frac{1}{\sqrt{\left(1 - \frac{(n_u, n_u)_{(t_s=0;t,t_w)}}{(u'_u, u'_u)_{(t_s=0;t,t_w)}}\right)\left(1 - \frac{(n_p, n_p)_{(t_s=0;t,t_w)}}{(u'_p, u'_p)_{(t_s=0;t,t_w)}}\right)}}. \tag{16}$$

This correction factor $c(t_s; t, t_w)$ depends on the unknown noise realizations $n_u(t)$ and $n_p(t)$. Note, that the correction factor only contains the zero-lag autocorrelations of these unknown noise realizations, and that, therefore, only an estimate of their respective variances is necessary to calculate the correction factor. In practice, assuming the noise is stationary, we can estimate these variances using the recorded wavefields $u'_u(t)$ and $u'_p(t)$ before $t = 0$ of the experiment. Replacing $n_u(t)$ and $n_p(t)$ in eq. (16) with the recorded wavefields before $t = 0$ is a good approximation only if the terms of the form $(u, n)_{(t_s;t,t_w)}$ and $(n_u, n_p)_{(t_s;t,t_w)}$ in eqs (8)–(10) are small compared to the remaining terms. Hence, for this replacement to be valid, we want the following inequalities to hold:

$$|(u_u + n_u, n_p)_{(t_s;t,t_w)} + (u_p, n_u)_{(t_s;t,t_w)}| \ll |(u_u, u_p)_{(t_s;t,t_w)}|, \tag{17}$$

$$2|(u_u, n_u)_{(t_s=0;t,t_w)}| \ll |(u_u, u_u)_{(t_s=0;t,t_w)} + (n_u, n_u)_{(t_s=0;t,t_w)}|, \tag{18}$$

$$2|(u_p, n_p)_{(t_s=0;t,t_w)}| \ll |(u_p, u_p)_{(t_s=0;t,t_w)} + (n_p, n_p)_{(t_s=0;t,t_w)}|, \tag{19}$$

where we have used the linearity of the $(\cdot, \cdot)_{(t_s;t,t_w)}$ in eq. (17). In Appendix A, we rewrite these three inequalities into one inequality that can be evaluated using only the noise-contaminated signals $u'_u(t)$ and $u'_p(t)$, and a representative noise realization $n_0(t)$, for example, estimated from the wavefields before $t = 0$ of the experiment. The resulting inequality [eq. (A5)] then determines if a certain time window has a reliable correction factor associated with it, when the unknown noise signals $n_u(t)$ and $n_p(t)$ in eq. (16) are replaced with $n_0(t)$. Since for the applications treated in this work, (i.e. a displacement of the source and the displacement of the scatterer locations) the maximum correlation occurs at time-shift $t_s = \langle\tau\rangle = 0$ s, we treat the special case $t_s = 0$ in Appendix A only.

Replacing $n_u(t)$ and $n_p(t)$ with $n_0(t)$ in eq. (16), the correction factor is given by

$$c(t_s; t, t_w) \approx \frac{1}{\sqrt{\left(1 - \frac{(n_0, n_0)_{(t_s=0;t,t_w)}}{(u'_u, u'_u)_{(t_s=0;t,t_w)}}\right)\left(1 - \frac{(n_0, n_0)_{(t_s=0;t,t_w)}}{(u'_p, u'_p)_{(t_s=0;t,t_w)}}\right)}}, \tag{20}$$

and is considered reliable if inequality (A5) is satisfied with an appropriate value of γ [i.e. $O(10^{-1})$]. To derive condition (A5), we assume that the noise is stationary and that $n_u(t)$ and $n_p(t)$ have about the same noise levels, (i.e. the same variance). If the noise levels of $n_u(t)$ and $n_p(t)$ are substantially different, separate estimates of the variances $(n_u, n_u)_{(t_s=0;t,t_w)}$ and $(n_p, n_p)_{(t_s=0;t,t_w)}$ can be used in eq. (16) to calculate the correction factor. In this case condition (A5) does not apply, and a new condition could be derived. To avoid belabouring the point, we refrain from such a treatment.

4 DISPLACEMENT OF THE SCATTERERS

The problem of inferring the average displacement of scatterers in a strongly scattering medium from the multiply scattered wavefields, has been used to study fluidized particle suspensions (Weitz & Pine 1993; Heckmeier & Maret 1997; Page *et al.* 1999; Cowan *et al.* 2000; Page *et al.* 2000; Cowan *et al.* 2002). In geophysics, this problem may be relevant when a strongly scattering region in the earth is strained, causing the scattering heterogeneities to move. In such a situation the displacement of the scatterers is not expected to be random, but will be correlated among scatterers. Here, we present a numerical experiment with point scatterers in a homogeneous background model, where we randomly perturb the scatterer locations and use CWI to infer their rms displacement. Although this experiment is not directly related to a changing strain in the earth, it serves the purpose of testing the workings of our correction factor.

Snieder & Scales (1998) showed that for independent perturbations of the scatterer positions and isotropic scattering, the variance of the path length L is given by

$$\sigma_L^2 = 2n\delta^2, \tag{21}$$

where n is the number of scatterers along the path, and δ is the rms displacement of the scatterers in the direction of either coordinate axis (horizontal and vertical for two dimensions). Note that Snieder and Scales assume all directions of random displacement to be equally likely. As a result, the rms displacement is the same in each direction (horizontal and vertical for 2-D), that is, for 2-D the true rms displacement would be $\sqrt{2}\delta$. Using that the number of scatterers is on average given by $n = vt/l^*$, with l^* the transport mean free path (Lagendijk & van Tiggelen 1996) and v the velocity, and using $L = vt$, it follows that the variance of the traveltime perturbations is given by

$$\sigma_\tau^2 = \frac{2\delta^2 t}{vl^*}. \tag{22}$$

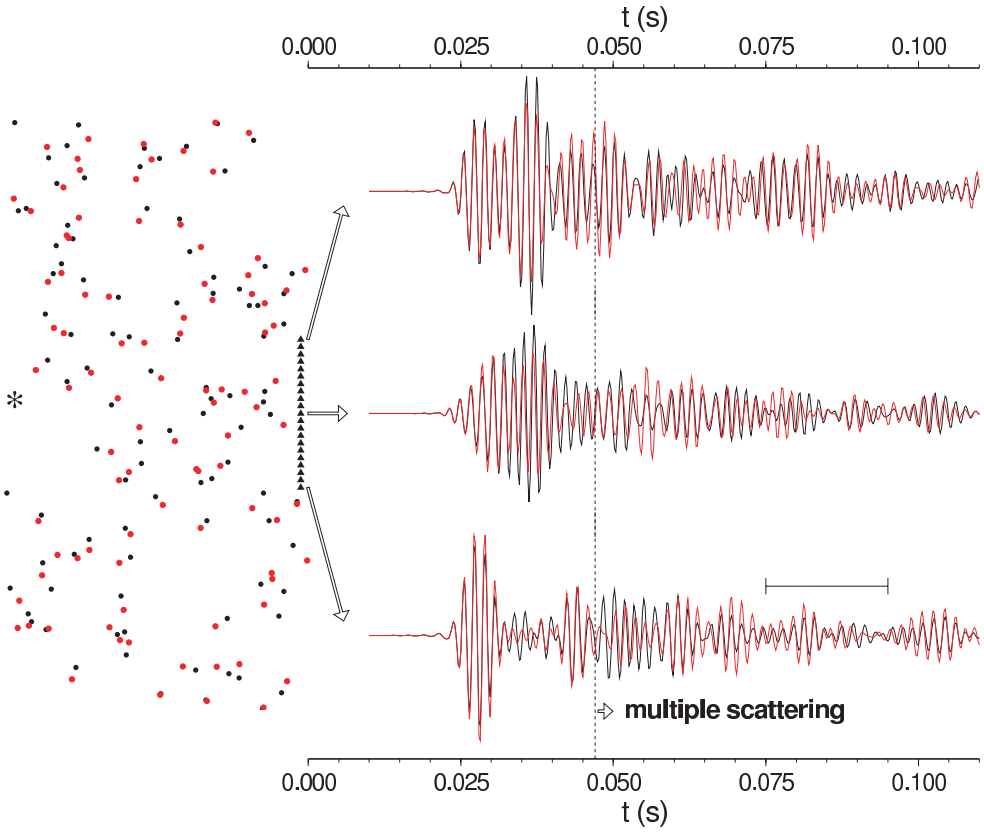

Figure 1. Unperturbed (black) and perturbed (red) locations of the point scatterers in the medium. For display purposes the differences between the unperturbed and perturbed locations are magnified by a factor 10. The star denotes the source and the triangles the receivers. The modelled seismograms are shown for three receivers. The black seismograms are related to the unperturbed scatterer locations, and the red seismograms to the perturbed locations. For times later than $t = 4.7 \times 10^{-2}$ s (marked by the dotted line), the waves have scattered more than four times. The horizontal bar indicates the window length for the time-windowed cross-correlations used to calculate the rms displacement δ shown in Fig. 2.

Inserting this in eq. (2), it follows that the rms displacement δ can be found from

$$\delta = \sqrt{(1 - \max[r(t_s; t, t_w)])\frac{vl^*}{\omega^2 t}}. \tag{23}$$

Since the perturbations of the scatterer locations are assumed to be independent, and since the scattering is assumed to be isotropic, the mean traveltime perturbation $\langle \tau \rangle = 0$. This means that the maximum of the time-windowed cross-correlation function occurs at zero lag, that is, $t_s = 0$.

Fig. 1 shows the setup of our numerical experiment to test the inference of the scatterer displacements from the seismic coda using eq. (23). This experiment was also outlined in Snieder *et al.* (2002). 100 point scatterers (black dots) are contained in an area of 40×80 m^2, and the waveforms are calculated using a numerical implementation (Groenenboom & Snieder 1995) of Foldy's method (Foldy 1945). The resulting seismograms are shown by the black lines for three locations on the edge of the area, and the source location is indicated by the asterisk. In these calculations the scattering amplitude was set to $-4i$, in order to get the maximum possible scattering strength as constrained by the optical theorem [Groenenboom & Snieder (1995); in their notation we used $\gamma = 4$]. The background velocity equalled 1500 m s^{-1} and the source spectrum $S(\omega) = e^{-\omega^2/\omega_0^2}$, with ω the angular frequency, $\omega_0 = 2\pi f_0$, and $f_0 = 600$ Hz. The frequency band used was 400–800 Hz, with a resulting dominant frequency of about 500 Hz due to tapering on either side of the spectrum. Since in our experiment we have isotropic scattering, the transport mean free path equals the mean free path, that is, $l^* = l$. The mean free path in our simulation was measured to be $l = 17.6$ m, which, using $n = vt/l$, can be used to infer that after $t = 4.7 \times 10^{-2}$ s the waves are on average scattered more than four times. This time is indicated in Fig. 1 by the dotted vertical line. The perturbed scatterer locations are indicated by the red dots in Fig. 1. For display purposes the displacements are magnified by a factor 10. The actual rms displacement is $\delta_{\text{true}} = 8 \times 10^{-2}$ m in both the horizontal and vertical direction. *This displacement equals just 1/38 of the dominant wavelength* (the dominant wavelength $\lambda = 3$ m). The resulting waveforms calculated using the displaced scatterers are shown for three receivers by the red lines.

Fig. 2(a) shows the inferred value of δ [using eq. (23)] as a function of the central window time t, where the estimated values for δ from all 21 receivers were averaged. (The receiver spacing was chosen such that the calculated multiply scattered waveforms were uncorrelated, meaning they can be treated as independent.) The dotted lines show the average inferred value of δ as a function of time plus or minus one standard deviation. The half-window duration t_w was 10^{-2} s, resulting in a window length of 10 dominant periods,

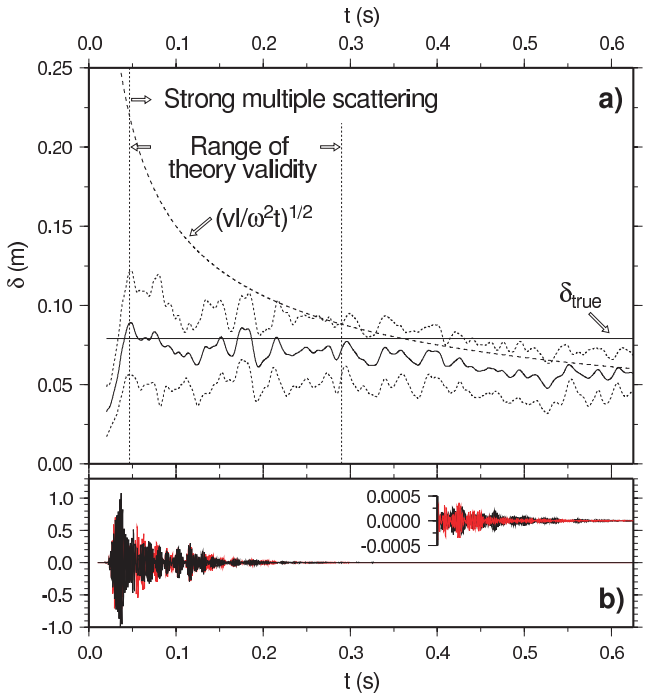

Figure 2. (a) Inferred rms displacement δ as a function of the centre window time t (solid line) plus or minus one standard deviation (dotted lines). The true value of δ is indicated by the horizontal solid line. The range of validity of CWI is indicated by the vertical dashed lines. The half-window time t_w used in calculating the time-windowed correlation coefficient equals 0.01 s. (b) Unperturbed (black) and perturbed (red) seismogram from the centre receiver seen in Fig. 1; the inset shows a blow-up of the seismograms for $t > 0.4$ s.

and $\sqrt{\overline{\omega^2}} = 3.66 \times 10^3\,\mathrm{rad\,s^{-1}}$. The vertical dashed lines indicated the range of validity of eq. (23). For early times (i.e. $t < 4.7 \times 10^{-2}$ s) the relation $n = vt/l$ for the number of scatterings used in the derivation of eq. (23) is not valid, and for late times (i.e. $t > 2.9 \times 10^{-1}$ s), the second-order Taylor approximation of the autocorrelation of the source signal is inaccurate by more than 15 per cent. This latter time is indicated by the rightmost dotted vertical line in Fig. 2. For reference, Fig. 2(b) shows an unperturbed (black) and perturbed (red) wavefield from the centre receiver seen in Fig. 1; the inset shows a blow-up of the seismograms at late times, indicating that the signal is small, yet well above numerical precision.

Within the range of validity of eq. (23), Fig. 2(a) shows that the true displacement is recovered within the range given by the average rms displacement plus or minus one standard deviation. For late times, the correlation coefficient is close to zero and, according to eq. (23), the inferred value of δ is then given by $\sqrt{vl/(\overline{\omega^2}t)}$. This function is indicated by the dashed line in Fig. 2 and agrees well with the inferred value of δ for late times. For these times the inferred value of δ is of course no longer a good estimate of the true rms displacement.

As mentioned in the introduction, when the wavefields are contaminated with noise, the number of independent time windows that can be used is limited to traveltimes where the ambient noise level is small compared to the amplitudes of the multiply scattered waves. In order to be able to use as many independent time windows as possible, and hence reduce the error bars on the inferred perturbation, it is important to correct the cross-correlation function for the bias due to the noise. To test the correction factor in eq. (20), we added band-limited noise to the waveforms for all 21 receivers from our numerical experiment. The bandwidth of the noise was the same as that of the noise-free signals (i.e. 400–800 Hz). Fig. 3 shows a waveform with and without the added noise. Using the noise-contaminated waveforms, we again calculated the

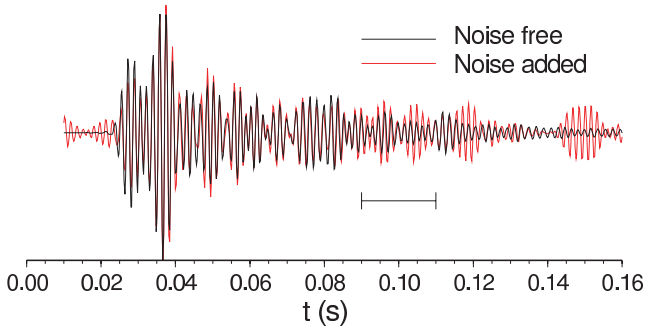

Figure 3. An example signal without noise (black) and with noise (red). The horizontal bar indicates the window length for the time-windowed cross-correlations used to calculate the rms displacement δ shown in Fig. 4.

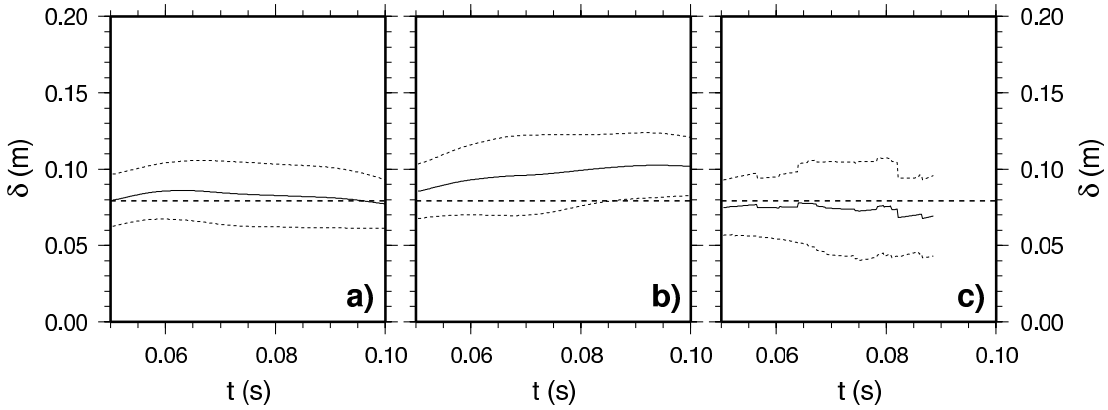

Figure 4. Inferred value of δ as a function of the central window time t, obtained using eq. (23) with (a) the noise-free signals, (b) the noise-contaminated signals but no application of the correction factor and (c) the noise-contaminated signals with application of the correction factor using eq. (20).

inferred values of δ both with and without the correction factor; see Figs 4(c) and (b) respectively. For reference, Fig. 4(a) shows the inferred value of δ when the noise-free signals were used. Fig. 4(b) shows that the noise induces a bias in the estimated value of δ; the presence of noise reduces the correlation between the unperturbed and perturbed waveforms, and causes the inferred values of δ, calculated using eq. (23), to be larger. For early times, the true value of δ is embedded within the average value of δ plus or minus one standard deviation, but the estimated average value of δ is too high, especially for later times, where the lower amplitude values of the coda result in lower signal-to-noise ratios. Fig. 4(c) shows that the correction factor from eq. (20) accurately accounts for the bias due to the noise. The noise estimates were obtained using the signal before the main first arrival in the seismograms. In the calculation of the results shown in Fig. 4(c), we used condition (A5) for each receiver, with $\gamma = 0.125$ to select the time windows used for the inversion of δ (note that this is a different γ than that used by Groenenboom & Snieder (1995), where γ determines the scattering strength). As a result, the number of receivers that had usable time windows for a given central window time t, varies for different t. This causes the jagged appearance of the average inferred value of δ (and the standard deviation). We used a time window only when at least seven receivers (i.e. 30 per cent of the receivers) satisfied condition (A5) at the central window time t. After $t \approx 9 \times 10^{-2}$ s fewer than seven time windows satisfied condition (A5) with $\gamma = 0.125$, and hence the correction factor was judged unreliable. As a result, the noise-corrected estimates of the rms displacement are not shown for times larger than $t \approx 9 \times 10^{-2}$ s.

5 SOURCE SEPARATION

Snieder & Vrijlandt (2005) used CWI to estimate the distance between seismic events recorded at a single station, that have the same source mechanism. They derive the imprint of a change in source location on the variance of the traveltime differences, and then use equation (2) to infer this change from the maximum of the cross-correlation function, that is, max $[r(t_s; t, t_w)]$. In addition they show that for a change in source location this maximum occurs at time-shift $t_s = \langle \tau \rangle = 0$, and that for two double-couple sources with a source separation in the fault plane, the relation between the source displacement Δs and the variance of the traveltimes σ_τ^2 is given by

$$\sigma_\tau^2 = \frac{\left(\frac{6}{\alpha^8} + \frac{7}{\beta^8}\right)}{7\left(\frac{2}{\alpha^6} + \frac{3}{\beta^6}\right)} (\Delta s)^2, \tag{24}$$

where α and β are the P and S wave velocities, respectively. Different non-overlapping time windows provide independent estimates of the source separation. These independent estimates in turn allow for the calculation of error estimates of the source separation.

Fig. 5(a) shows two seismograms (events 242003 and 242020) from earthquakes on the Hayward fault, California (Waldhauser & Ellsworth 2000), recorded at station CSP of the Northern California Seismic Network. The recorded signal before the arrival of the P wave shows that the noise level is considerable. Fig. 5(b) shows the maximum of the time-windowed cross-correlation function without the correction factor (thin line) and with the correction factor (thick line) applied, and Fig. 5(c) shows the inferred values of the source separation using eq. (24). Here the noise level (or variance) was estimated from the waveforms before the first arrivals. The half-window duration t_w used is 5 s (the full-window length is indicated by the horizontal bar in Fig. 5a), and the P and S wave velocities used to calculate the source displacement are $\alpha = 5750$ m s^{-1} and $\beta = 3320$ m s^{-1}, respectively. Note that we used overlapping time windows, since we plot max $[r(t_s; t, t_w)]$ simply as a continuous function of the central window time t. Of course, non-overlapping windows could be used to ensure independent estimates of the source separation.

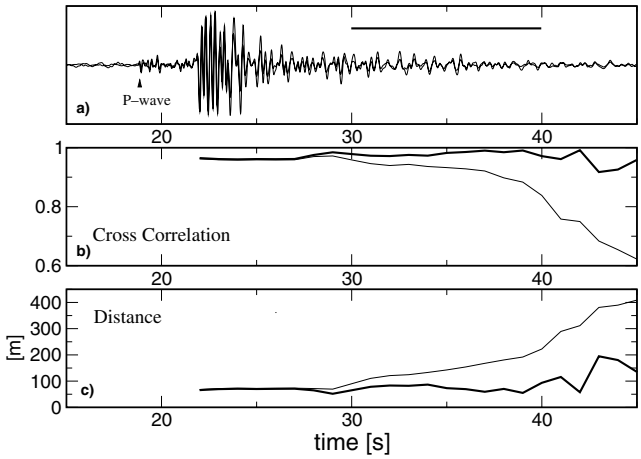

Figure 5. Two seismograms from two earthquakes on the Hayward fault, California, recorded at station CSP of the Northern California Seismic Network (a), their cross-correlation maximum max $[r(t_s; t, t_w)]$ as a function of the central window time t (b), uncorrected (thin line) and corrected (thick line) and the inferred source displacement (c) using both the uncorrected (thin line) and corrected (thick line) values of max $[r(t_s; t, t_w)]$ shown in (b). The horizontal line in (a) indicates the window length used in the cross-correlation.

Fig. 5(b) shows that the corrected values of max $[r(t_s; t, t_w)]$ maintain a fairly constant level for times t late in the coda, whereas the uncorrected values decrease earlier in the coda because the noise decreases the similarity between both waveforms. As a result, the inferred values of the source separation using eq. (24) are more or less constant for larger traveltimes when the corrected values of max $[r(t_s; t, t_w)]$ are used (Fig. 5c). This indicates that the correction factor $c(t_s; t, t_w)$ given by eq. (20), accurately corrects for the influence of the noise on the cross-correlation function. For very large times (say $t > 40$ s) the corrected values are more variable because the correction factor becomes unreliable. We purposely showed the times where the corrected values become variable, to indicate the level of variation caused by an unreliable correction factor. Of course, the time where the correction factor becomes unreliable could have been estimated using condition (A5) with an appropriate value of γ [i.e. $O(10^{-1})$].

6 CONCLUSION

We have derived a correction factor for the influence of noise on the cross-correlation function, and have shown its accuracy using both numerical and field data. The derivation of the correction factor is based on the assumption that the stochastic processes underlying the noise realizations in both the unperturbed and perturbed signal, are mutually uncorrelated and stationary with zero mean. We show the application of this correction factor in the context of CWI, for the inference of the rms displacement of scatterers and a displacement of the source, from multiply scattered wavefields. For the displacement of the scatterers, we showed that in the presence of noise, a displacement of *only* 1/38 *from the dominant wavelength* can be successfully retrieved from the cross-correlation between the unperturbed and perturbed signals. This shows the power of CWI when compared to methods that use singly scattered waves only.

Both in case of a displacement of the scatterer locations and in case of a change in the source location, the perturbation is independent of the traveltimes of the multiply scattered waves. Using non-overlapping time windows to estimate the perturbations provides a consistency check of the method, and allows the calculation of error estimates. Therefore, our correction factor is relevant, as it increases the number of usable time windows and hence allows for a reduction of the error estimates. In addition, the correction factor adjusts for bias in the cross-correlation induced by the noise. Since our factor depends on an estimate of the noise level in the data, we present a condition that allows determination of the reliability of the correction for a zero-lag cross-correlation. This condition can be verified using only noise-contaminated signals and an estimate of the noise level in the data. Using this condition, the time windows used in the zero-lag time-windowed cross-correlation can be judged to be reliable or not.

The use of the proposed correction factor is of course not limited to CWI. Any application that uses cross-correlations between different and noisy signals, and needs to correct for bias induced by noise, can benefit from the correction factor presented here.

ACKNOWLEDGMENTS

We thank Mark Vrijlandt for Fig. 5, and Ken Larner and two anonymous reviewers for their critical reviews. In addition, we thank Western Geophysical (now WesternGeco), and in particular Peter Nuttall, for funding a 3-month visit of HD to the Center for Wave Phenomena at the Colorado School of Mines. This work was supported by the NSF (grant EAR-0106668) and by the sponsors of the Consortium Project on Seismic Inverse Methods for Complex Structures at the Center for Wave Phenomena.

REFERENCES

Cowan, M., Page, J. & Weitz, D., 2000. Velocity fluctuations in fluidized suspensions probed by ultrasonic correlation spectroscopy, *Phys. Rev. Lett.,* **85,** 453–456.

Cowan, M., Jones, I., Page, J. & Weitz, D., 2002. Diffusing acoustic wave spectroscopy, *Phys. Rev. E,* **65,** 066605–1/11.

Derode, A., Roux, P. & Fink, M., 1995. Robust acoustic time reversal with high-order multiple scattering, *Phys. Rev. Lett.,* **75,** 4206–4209.

Derode, A., Tourin, A. & Fink, M., 1999. Ultrasonic pulse compression with one-bit time reversal through multiple scattering, *J. Appl. Phys.,* **85,** 6343–6352.

Fink, M., 1997. Time-reversed acoustics, *Physics Today,* **50,** 34–40.

Foldy, L., 1945. The multiple scattering of waves, *Phys. Rev.,* **67,** 107–119.

Grêt, A., Snieder, R., Aster, R. & Kyle, P., 2005a. Monitoring rapid temporal changes in a volcano with coda wave interferometry, *Geophys. Res. Lett.,* **32,** L06304, 10.1029/2004GL021143.

Grêt, A., Snieder, R. & Scales, J., 2005b. Time-lapse monitoring of rock properties with coda wave interferometry, Submitted to *J. geophys. Res.*.

Groenenboom, J. & Snieder, R., 1995. Attenuation, dispersion, and anisotropy by multiple scattering of transmitted waves through distributions of scatterers, *J. acoust. Soc. Am.,* **98**(6), 1–11.

Heckmeier, M. & Maret, G., 1997. Dark speckle imaging of colloidal suspensions in multiple light scattering media, *Progr. Colloid. Polym. Sci.,* **104,** 12–16.

Lagendijk, A. & van Tiggelen, B., 1996. Resonant multiple scattering of light, *Phys. Rep.,* **270,** 143–215.

Maret, G. & Wolf, G., 1987. Effect of brownian motion of scatterers, *Z. Phys. B,* **65,** 409–413.

Page, J., Jones, I., Schriemer, H., Cowan, M., Sheng, P. & Weitz, D., 1999. Diffusive transport of acoustic waves in strongly scattering media, *Physica B,* 263–264, 37.

Page, J., Cowan, M. & Weitz, D., 2000. Diffusing acoustic wave spectroscopy of fluidized suspensions, *Physica B,* **279,** 130–133.

Papoulis, A., 1991. *Probability, Random Variables, and Stochastic Processes*, McGraw-Hill Inc.

Pine, D., Weitz, D., Chaikin, P. & Herbolzheimer, E., 1988. Diffusing wave spectroscopy, *Phys. Rev. Lett.,* **60,** 1134–1137.

Roberts, P., Scott Phillips, W. & Fehler, M., 1992. Development of the active doublet method for measuring small velocity and attenuation changes in solids, *J. acoust. Soc. Am.,* **91,** 3291–3302.

Snieder, R., 2002. Coda wave interferometry and the equilibration of energy in elastic media, *Phys. Rev. E,* **66,** 046615–1, 8.

Snieder, R., 2004. Coda wave interferometry, in *2004 McGraw-Hill yearbook of science & technology*, pp. 54–56, McGraw-Hill, New York.

Snieder, R., 2006. The theory of coda wave interferometry, *Pure appl. Geophys.,* in press.

Snieder, R. & Scales, J., 1998. Time reversed imaging as a diagnostic of wave and particle chaos, *Phys. Rev. E,* **58,** 5668–5675.

Snieder, R. & Vrijlandt, M., 2005. Constraining relative source locations with coda wave interferometry: theory and application to earthquake doublets in the Hayward Fault, California, *J. Geophys. Res.,* **110,** B04301, 10.1029/2004JB003317.

Snieder, R., Grêt, A., Douma, H. & Scales, J., 2002. Coda wave interferometry for estimating nonlinear behavior in seismic velocity, *Science,* **295,** 2253–2255.

Waldhauser, F. & Ellsworth, W., 2000. A double-difference earthquake location algorithm: method and application to the northern Hayward fault, California, *Bull. seism. Soc. Am.,* **90,** 1353–1368.

Weitz, D. & Pine, D., 1993. Diffusing wave spectroscopy, in *Dynamic Light Scattering*, p. 652, ed. Brown, W., Clarendon Press, Oxford.

Yodh, A., Kaplan, P. & Pine, D., 1990. Pulsed diffusing-wave spectroscopy: high resolution through nonlinear optical gating, *Phys. Rev. B,* **42,** 4744–4747.

APPENDIX A: A CONDITION TO ESTIMATE THE RELIABILITY OF THE ZERO-LAG CROSS-CORRELATION CORRECTION FACTOR

Eq. (16) for the correction factor of the cross-correlation coefficient, depends on the unknown noise functions $n_u(t)$ and $n_p(t)$. In practice, we do not know these noise functions and often only have an estimate of the noise level, as opposed to some ensemble average. We want the correction factor to be reliable when the unknown variances of the noise in eq. (16) are replaced by a single estimate of the noise level. If inequalities (17)–(19) are satisfied, the correction factor depends only weakly on the estimate of the noise level. Here we rewrite these inequalities into one inequality that can be verified using the noise-contaminated signals and an estimate of a single realization of the noise $n_0(t)$.

To write inequalities (17)–(19) as a single one, we first add the left- and right-hand sides of eqs (17)–(19), while multiplying eq. (17) by two for convenience in the further derivation. This gives

$$2(|(u_u + n_u, n_p)_{(t_s;t,t_w)} + (u_p, n_u)_{(t_s;t,t_w)}| + |(u_u, n_u)_{(t_s=0;t,t_w)}| + |(u_p, n_p)_{(t_s=0;t,t_w)}|)$$
$$\ll$$
$$2|(u_u, u_p)_{(t_s;t,t_w)}| + (u_u, u_u)_{(t_s=0;t,t_w)} + (n_u, n_u)_{(t_s=0;t,t_w)} + (u_p, u_p)_{(t_s=0;t,t_w)} + (n_p, n_p)_{(t_s=0;t,t_w)}, \quad \text{(A1)}$$

where we have used that zero-lag autocorrelations are positive definite. If conditions (17)–(19) hold, eqs (13)–(15) from the main text are good approximations. We can use these approximations, together with the linearity of $(\cdot\,,\cdot)_{(t_s;t,t_w)}$ and eq. (5), to approximate inequality (A1) as

$$2|(u'_u, n_p)_{(t_s;t,t_w)} + (u'_p, n_u)_{(t_s;t,t_w)} - (n_u, n_p)_{(t_s;t,t_w)}|$$
$$+ 2|(u'_u, n_u)_{(t_s=0;t,t_w)} - (n_u, n_u)_{(t_s=0;t,t_w)}| + 2|(u'_p, n_p)_{(t_s=0;t,t_w)} - (n_p, n_p)_{(t_s=0;t,t_w)}|$$
$$\ll$$
$$2|(u'_u, u'_p)_{(t_s;t,t_w)}| + (u'_u, u'_u)_{(t_s=0;t,t_w)} + (u'_p, u'_p)_{(t_s=0;t,t_w)}. \quad \text{(A2)}$$

For the applications treated in this paper, that is, a source displacement and the displacement of the scatterer locations, the maximum cross-correlation occurs for $t_s = \langle\tau\rangle = 0$ s. Also, since in CWI we assume that the travel-time perturbations in the time window $[t - t_w, t + t_w]$ are small, we expect a positive cross-correlation between the signals $u'_u(t)$ and $u'_p(t)$ for times where CWI is valid. Hence, making

use of this approximation, and setting $t_s = 0$ in condition (A2), we can write this condition as

$$|(u'_u + u'_p, n_0)_{(t_s=0;t,t_w)}| + |(u'_u, n_0)_{(t_s=0;t,t_w)} - (n_0, n_0)_{(t_s=0;t,t_w)}| \ldots$$
$$+|(u'_p, n_0)_{(t_s=0;t,t_w)} - (n_0, n_0)_{(t_s=0;t,t_w)}| \ll 2([u'_u + u'_p]/2, [u'_u + u'_p]/2)_{(t_s=0;t,t_w)} \quad \text{(A3)}$$

where we substituted for both noise signals $n_u(t)$ and $n_p(t)$ the estimated noise signal $n_0(t)$, and we assumed $|(n_u, n_p)_{(t_s;t,t_w)}| \ll |(u'_u, n_p)_{(t_s;t,t_w)} + (u'_p, n_u)_{(t_s;t,t_w)}|$ to eliminate the $(n_u, n_p)_{(t_s;t,t_w)}$ term. The latter approximation is more appropriate for larger signal-to-noise ratios, larger time windows, and uncorrelated noise realizations $n_u(t)$ and $n_p(t)$. Note that substituting a single noise signal for both unknown noise signals $n_u(t)$ and $n_p(t)$ is appropriate only if both noise signals have similar noise levels. Dividing both sides of condition (A3) by $(n_0, n_0)_{(t_s=0;t,t_w)}$ (which is positive definite), and defining the ratio

$$\Gamma(t, t_w) := \frac{([u'_u + u'_p]/2, [u'_u + u'_p]/2)_{(t_s=0;t,t_w)}}{(n_0, n_0)_{(t_s=0;t,t_w)}}, \quad \text{(A4)}$$

inequality (A3) leads to

$$\frac{1}{2}\left(\left|\frac{(u'_u + u'_p, n_0)_{(t_s=0;t,t_w)}}{(n_0, n_0)_{(t_s=0;t,t_w)}}\right| + \left|\frac{(u'_u, n_0)_{(t_s=0;t,t_w)}}{(n_0, n_0)_{(t_s=0;t,t_w)}} - 1\right| + \left|\frac{(u'_p, n_0)_{(t_s=0;t,t_w)}}{(n_0, n_0)_{(t_s=0;t,t_w)}} - 1\right|\right) / \Gamma(t, t_w) \leq \gamma, \quad \text{(A5)}$$

where γ is $O(10^{-1})$. Here $\sqrt{\Gamma(t, t_w)}$ can be interpreted as the average signal-to-noise ratio.

Condition (A5) is satisfied only for time windows that have a large average signal-to-noise ratio. The l.h.s of condition (A5) can be evaluated using the noise-contaminated signals $u'_u(t)$ and $u_p(t)$, and an estimated noise signal $n_0(t)$. This condition can thus be used as a selection criterion to determine which time windows have reliable correction factors associated with them, when an estimated noise level (calculated using an estimated noise realization $n_0(t)$) is used, that is, when eq. (20) is used to calculate the correction factor. Note that γ can be interpreted as the inverse of the signal-to-noise ratio.